

Quantitative Modeling of the Architecture and Connectivity Properties of Reservoirs in ‘Royal’ Field, Niger-Delta.

B.T Ojo^{*}, M.T Olowokere and M.I Oladapo

Department of Applied Geophysics, Federal University of Technology, Akure.

Corresponding Author: B.T Ojo

Abstract: A fit for purpose geologic model was constructed for reservoirs in ‘Royal’ field in order to carry out dynamic modelling and predict the future performance of the reservoirs. The sand continuity in the reservoirs were interrupted by the presence of shale streaks as signified by the Gamma Ray Log signatures and splitting effects on the peaks of the picked horizons. The modelled petrophysical parameters (porosity, water saturation and permeability) gave a better understanding of the reservoir properties. Reservoir B has an average effective porosity of 20% and a water saturation ranging from 10%-22%. Reservoir C has an average effective porosity of 22% and water saturation ranging from 17%-34%. It was also observed from the Rock Physics cross plot that the reservoirs cementing properties were low possibly due to the significantly low clay content. Two major faults were identified across the seismic section. From the results, possible location for future wells was suggested due to the observable increase in hydrocarbon content from Well D, South-Westwards towards well C on the four-way closure identified on the structural maps.

Keywords: Cementing Properties, Dynamic Modelling, Fluid Availability, Lithological Composition, Rock Physics.

Date of Submission: 17-03-2018

Date of acceptance: 02-04-2018

I. Introduction

Production of hydrocarbon involves a substantial amount of understanding of the reservoirs properties and behaviour. (Schlumberger. 1989). Logs help define physical rock characteristics such as lithology, porosity, pore geometry, and permeability. (Abe and Olowokere 2013.) Logging data is used to identify productive zones, to determine depth and thickness of zones, to distinguish between oil, gas, or water in a reservoir, and to estimate hydrocarbon reserves. (Edigbue et al 2014). Seismic data has better lateral variation and better resolution than well logs. (Alistair 2004). The amount of internal space or voids in a given volume of rock is the measure of the amount of fluids a rock will hold. The amount of void space that is interconnected to transmit fluids is called effective porosity and only isolated pores and pore volume occupied by adsorbed water are excluded from this. (Amigun J.O et al 2012). Permeability is the property a rock has to transmit fluids. It is related to porosity but is not always dependent upon it. It is also controlled by the size of the connecting passages (pore throats or capillaries) between pores. (Nwankwo 2014). Static modelling help in identifying and knowing how reservoir properties are being distributed within the subsurface. (Lukumon 2014), (Oluwadare et al 2017). Proper reservoir management involves application of available technology and knowledge to a reservoir system within a given environment in order to maximize economic recovery. (Ailin and Dongbo 2012). The aim of this study is to quantitatively model the reservoir properties for better understanding of its connectivity for future enhancement of hydrocarbon production on the field. For this study, 3D Seismic and well logs which include Gamma ray, Sonic, Density and Resistivity logs were used. Due to the unavailability of the necessary data set, only structural changes over time could be identified and utilized in this study. Neutron logs which is a porosity log that measure the hydrogen ion concentration in a formation was not available to identify the type of hydrocarbon present. Rock Physics crossplots were also used to predict fluid type, lithological as well as the cementing properties of the reservoirs.

II. Geology And Location The Study Area

‘ROYAL’ field is an offshore field located in Niger Delta in the southern part of Nigeria. (Figure 1). Niger Delta is a prolific hydrocarbon belt in the world. The formation of Niger Delta basin was initiated in the early Tertiary time. The Niger Delta is situated in the Gulf of Guinea and extends throughout the Niger Delta province. (Doust and Omotsola 1990) From the Eocene to the present, the Delta has prograded Southwest ward, forming depobelts that represent the most active portion of the Delta at each stage of its development. (Michele 1999). Deposition of the three formations occurred in each of the five off lapping siliciclastic sedimentation cycles that comprise the Niger Delta. These cycles (depobelts) are 30 - 60 kilometers wide, prograde

southwestward 250 kilometres over oceanic coast into the Gulf of Guinea and are defined by synsedimentary faulting that occurred in response to variable rates of subsidence and sediment supply. The Niger Delta is a regressive sequence of clastic sediments developed in a series of offlap cycles. (Kearey 2001). All deep wells in the basin document a tripartite litho-stratigraphic succession in which the regressive sequence is demonstrated. The uppermost (shallowest) part of the sequence is a massive non-marine sand section, known as the Benin Formation, deposited in alluvial or upper coastal plain environments. This grades downwards into interbedded shallow-marine and fluvial sands, silts and clays, which form the typical paralic facies portion of the delta. It is known as the Agbada Formation; it has delivered most of the oil produced in the Niger Delta to date. The Delta formed at the site of a rift triple junction related to the opening of the Southern Atlantic starting in the late Jurassic from interbedded marine shale of the lowermost Agbada formation and continuing into the cretaceous. The Delta proper began developing in the Eocene, accumulating sediments that now are over 10km thick. (Doust and Omatsola 1990). It contains three stratigraphic units, upper Benin formation, middle Agbada formation and the lower Akata formation. (Figure 2). The primary source rock is the upper Akata formation, the marine-shale facies of the Delta, with possibly contribution from interbedded marine shale of the lowermost Agbada formation. Oil is produced from sand-stone facies within the Agbada Formation, however, turbidite sand in the upper Akata Formation is a potential target in deep water offshore and possibly beneath currently producing intervals onshore. (Doust and Omatsola 1990). In the southeast offshore, the hydrocarbon-rich Agbada formation is further subdivided into Biafra, Rubble and Qua Iboe members. Within these, there are type sections with intra and inter-formational relationships, the Biafra is Early to late Miocene. The Rubble bed is dated Late Miocene. The Biafra member progrades from thick continental/fluvial sediments in the north into delta plain and delta front deposits in the south, eventually becoming prodelta deposits shale into Akata further south. (Stacher 1995).

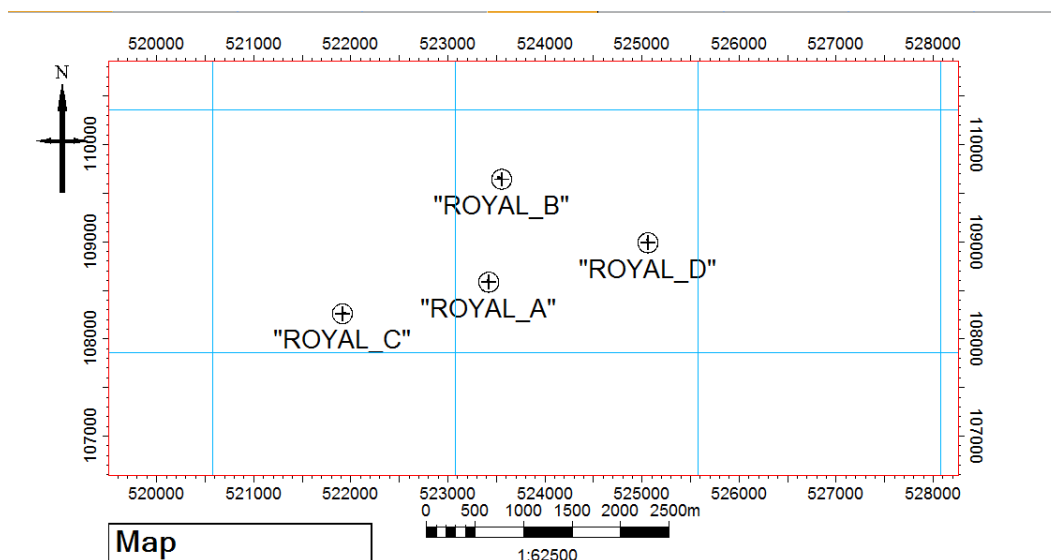


Figure 1: Base map of ROYAL field showing the well locations and seismic lines orientation

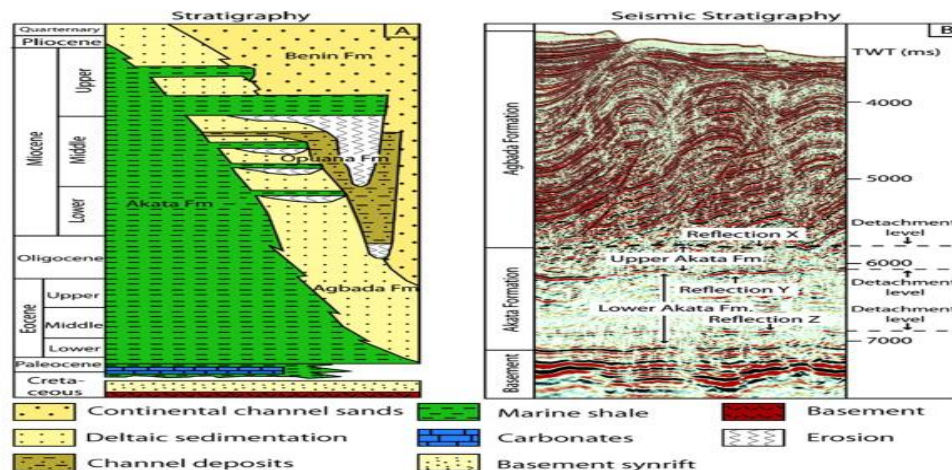


Figure 2: Stratigraphic Map of Niger Delta (Modified from Doust and Omatsola, 1990)

III. Materials And methodology.

MATERIALS.

The materials used in carrying out the research work include PETREL2013, ROK DOC. 3-D Seismic data and Well log data.

METHODOLOGY.

RESERVOIR GEOLOGY.

The lithology was delineated by first setting a range for the gamma ray log. The gamma ray log ranges from 0API to 150API. A cut-off limit of 75 API was used. Gamma ray logs measure natural radioactivity in formations and because of this measurement, they can be used for identifying lithologies and for correlating zones. The gamma ray log signature or measurement is based on the radioactive contents available in the formation. The gamma ray log will give a very high reading in shale formation due to the high radioactive content available in the formation, thus deflect to the right of the baseline while the sand formations will deflect to the left of the baseline due to the presence of quartz in the formation which has a low radioactive content. The correlation of the wells in 'Royal' field were carried out along the NE-SW direction. (Figure 3). With the aid of the resistivity log, two reservoirs (Reservoir B and Reservoir C) were identified across the field. The fluid maps reveal that the oil water contact (OWC) for reservoir B is at 5904.78 and oil water contact (OWC) for Reservoir C is at 6392.15. (Figure 4)

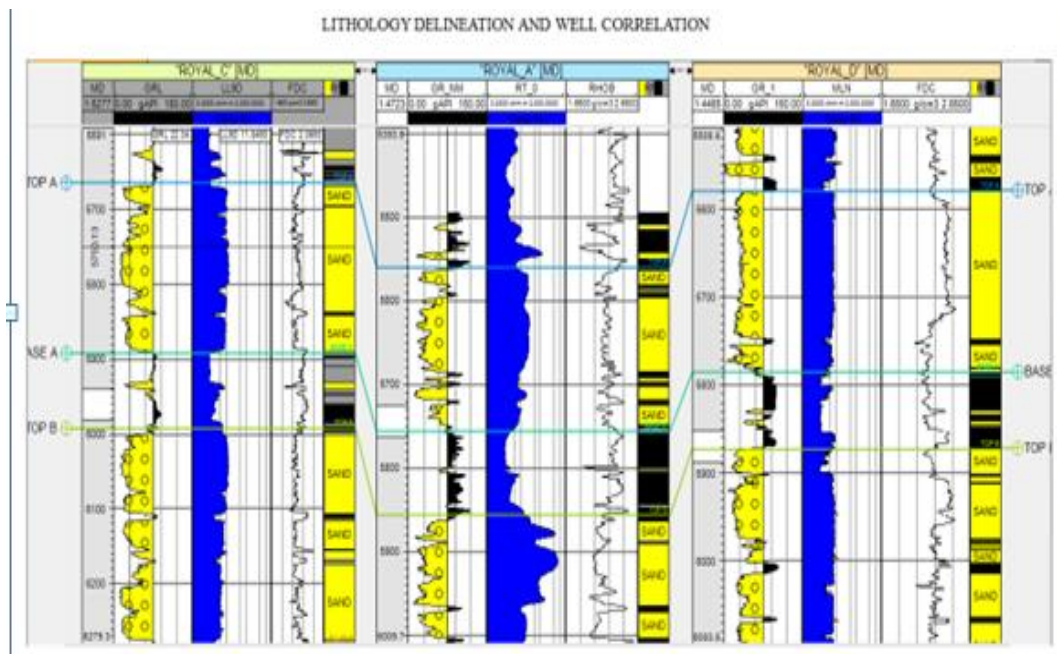


Figure 3: Lithology Delineation and Reservoir Identification along the NE-SW Direction

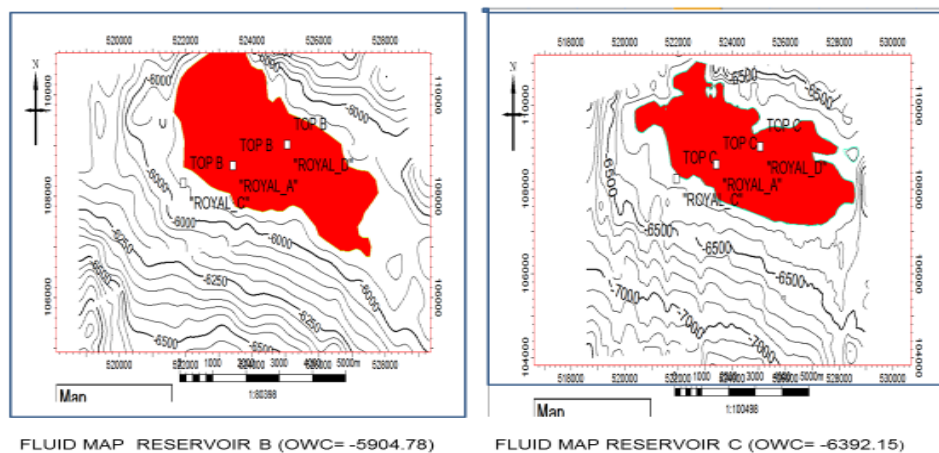


Figure 4: Fluid maps of reservoirs B and C showing the Oil Water Contact

IV. Seismicinterpretation

Prior to interpretation, the temporal positioning of the reservoirs of interest was determined on the base seismic data. The main geological units of interest are represented as seismic horizons corresponding to reservoir B and reservoir C respectively. Each of these horizons were identified within the seismic data through the correlation of the seismic reflection data with geological well data. It was observed that the synthetic trace with the well tops also tie very well on the seismic section. The reservoirs identified from the well correlation were related to seismic reflectors via synthetic seismograms. The synthetic seismogram (figure 5) were generated by the convolution of the reflection coefficient of each lithological unit with a ricker wavelet containing a frequency of 30Hz which is within the frequency range of the base seismic data. Prominent geologic structures such as major and minor faults was first identified across the seismic section. Two major faults were identified across the seismic section. The seismic events that correspond to the two reservoirs sand via the synthetic seismogram was mapped on the seismic reflections. The mapped horizons on the seismic were then contoured to generate a structural time map. The checkshot data which shows a relationship between the two-way time (TWT) and true vertical depth (TVD) was plotted against each other. A polynomial equation of the second order was derived from the plot. The equation was used to build a velocity model which was used to convert the structural time map to a structural depth map.

V. Static Model

In view of the necessity of dynamic simulation process and to arrive at a final well production and monitoring, it was necessary to build a static model that represent closely the subsurface reality of both reservoirs that have been encountered by the wells. The static geological model of reservoir B and reservoir C were built by integrating the structural interpretation from the base seismic data, petrophysical analysis from the well log data, and facies interpretation. The first stage in constructing a geologic model was to create a 3-D grid for the model. This was carried out via a process called pillargridding. Pillar Gridding is the process of making the ‘Skeleton Framework’ of the reservoir. The Skeleton is a grid consisting of a Top, a mid and Base skeleton grid. The aim of gridding in reservoir modelling is to turn the geological model of the field into a discrete system on which the fluid flow equations can be solved. The petrophysical parameters which is a continuous property was modelled using the Sequential Gaussian Stimulation.

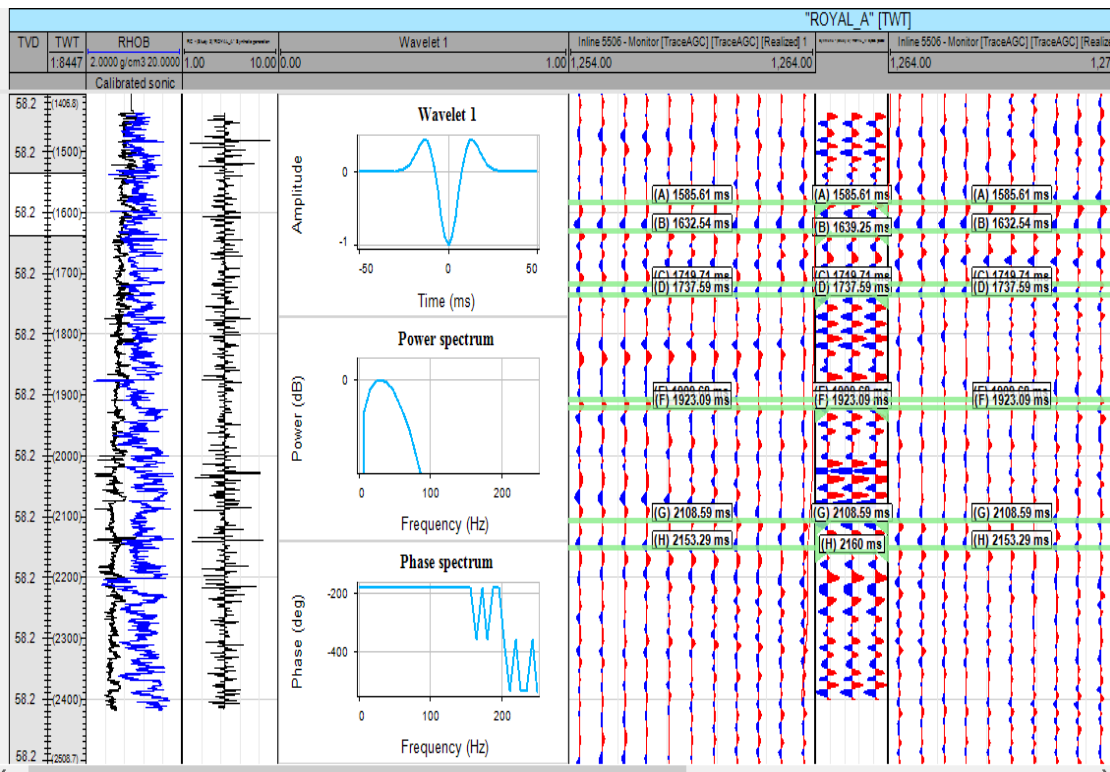


Figure 5: Synthetic Seismogram Generated from the Convolution of the Reflectivity Series and a Wavelet

VI. Rock Physics

Various Models were utilized in carrying out the rock physics analysis. A series of cross-plots were made using these models and the results were utilized in characterizing the reservoirs on the field. Specifically, they were used to further carry out fluid and lithology prediction and also an analysis of the degree of cementation of the lithologies within the reservoirs. The Cross-plots generated include:

i. Lambdarho-Murho Cross-plots

This was utilized for fluid prediction within the reservoirs. This plot is based on the fact that Lambdarho is a good fluid discriminating tool because it is higher in brine than in hydrocarbon bearing formations. From the plots, the abundance or lack of abundance of hydrocarbon in each well could be observed.

ii. Lambdarho-Velocity Ratio Cross-plots

Lambdarho being a better tool in separating shale from brine and hydrocarbon zones was utilized. The plots produced a similar result to that observed in lambdarho-murho cross-plots.

iii. Compressional Velocity-Porosity Cross-plots (Vp/Por)

This plot was used to map the degree of cementation within the reservoirs. Two models were used; The 'Contact Cement' and 'Friable Sand' Models.

iv. Compressional Velocity-Shear Velocity Cross-plots (Vp/Vs)

This plot was used to map lithology across the reservoirs. Two Models were used and they are the Greenberg-Castagna Sandstone and Shale models. The Compressional and Shear Wave velocities were generated using the equations below:

$$V_p = (1000000/DTc) * 0.3281 \quad (1)$$

$$V_s = (V_p - 1279.08)/1.11702 \quad (2)$$

Where V_p = Compressional Wave Velocity

V_s = Shear Wave Velocity

DTc = Compressional Sonic Log

Lambdarho and Murho were also generated from the Compressional and Shear Wave Velocities as shown below:

$$\lambda_p = Z_p - (2 * Z_s) \quad (3)$$

$$\mu_p = Z_s \quad (4)$$

Where λ_p = Lambda-rho

Z_p = Primary Impedance

Z_s = Secondary Impedance

μ_p = Mu-rho

μ = Shear Modulus

λ = Lamé's Constant

VII. Results And Discussion

RESERVOIR GEOLOGY

The well correlation of "Royal" field was carried out along NE-SW direction. One of the major reasons of carrying out correlation exercise within the given wells is to have an idea of the occurrences of horizontal sand packages from one well to the other that were deposited at the same time and space within the field. It was observed from the correlation panel that the sand packages are thinning towards the N-E direction. two prominent reservoirs identified are Reservoir B and Reservoir C. The non-availability of the Neutron log in any of the three wells makes it impossible to identify the fluid types (oil and gas) within these reservoirs. The Resistivity logs only help to indicate the presence of hydrocarbon within the field since they have high resistivity than water.

SEISMIC INTERPRETATION

The structural time map for the seismic data was generated for both reservoir B and C respectively (Figure 6a & 6b). From the structural time map of both reservoirs, it was observed that the map is having an anticlinal structure (four-way closure) which is of importance to the petroleum geologist, geophysicists and engineers since hydrocarbon can only accumulate within an anticlinal structure. The direction of the major fault is along the NE-SW. The other faults within this field are either synthetic or antithetic to the major faults. From the time map of reservoir B, it was also observed from the elevation legend that the orange colour indicate the shallowest part of the field while the light green colour indicate deepest part of the field. The contoured time values range from -1500ms to -1900ms. Also, from the time map of reservoir C, it was observed that the orange colour indicate the shallowest part of the field while the light green colour indicate deepest part of the field. The contoured time values range from -1640ms to -2100ms. The closure within this field is a four-way closure. The time maps above are also fault dependent which serve as a *seal* that prevent further migration of hydrocarbon. The velocity model (polynomial method) generated was used to convert the structural time map to a structural

depth map. The polynomial equation derived from the plot of Z against TWT was used to convert the time values on the structural time map to a depth values. From the structural depth maps of the seismic (Figure 7a & 7b), it was observed that there was no difference between both the structural time map and the structural depth map. The structural depth maps above are also a four-way closure (anticlinal structure) which is of interest to the petroleum geologist and reservoir engineers. The major faults also orientate in the same direction as that of the major faults on the time maps.

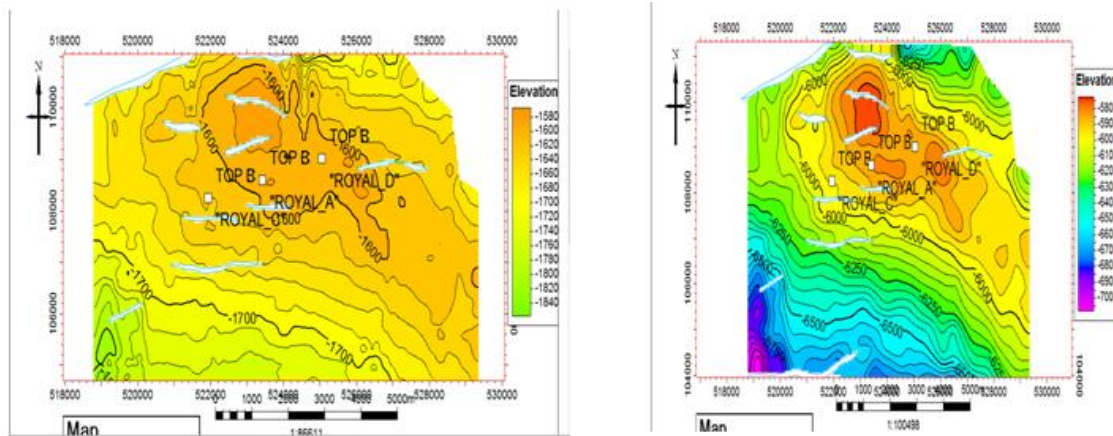


Figure 6a: Structural Time Map for Reservoir B Figure 7a: Structural Depth Map for Reservoir B

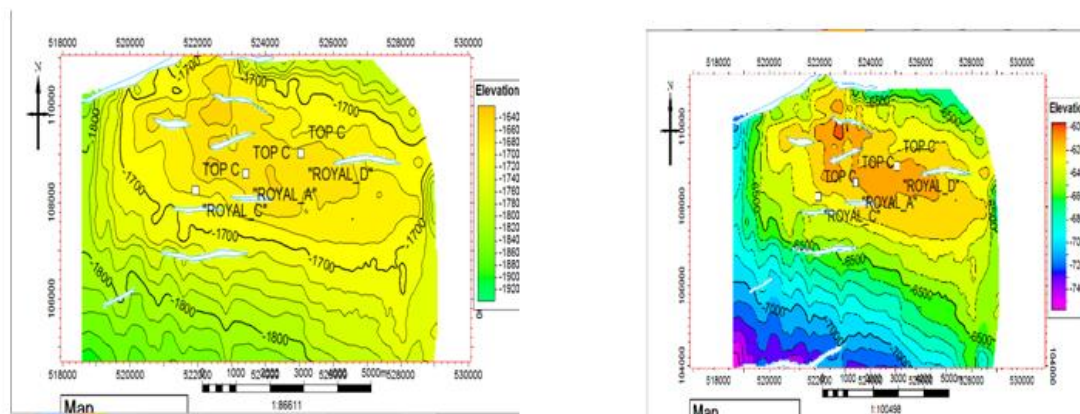


Figure 6b: Structural Time Map for Reservoir C Figure 7b: Structural Depth Map for Reservoir C

From the structural maps (reservoir B and reservoir C) the closure observed was a four-way closure. This trap and prevent further migration of hydrocarbon within the reservoirs.

STATIC MODEL

The average effective porosity of reservoir B is 20% (figure 8). This indicate the pore spaces within this reservoir are well connected. The water saturation within this reservoir ranges from 10%-17% (figure 9 and figure 10). This implies that the reservoir was highly saturated with hydrocarbon.

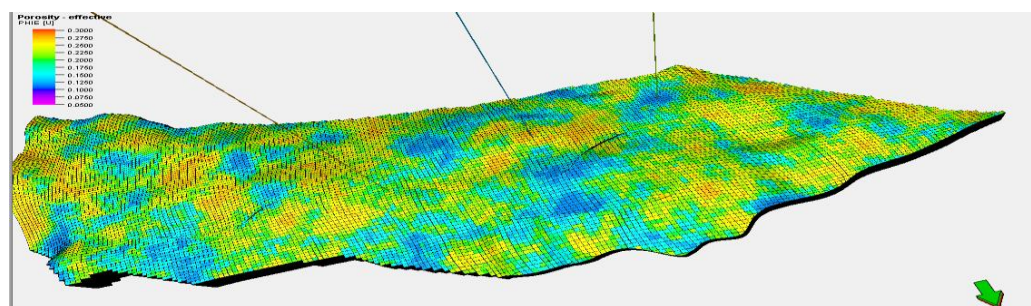


Figure 8: Effective Porosity Model for Reservoir B

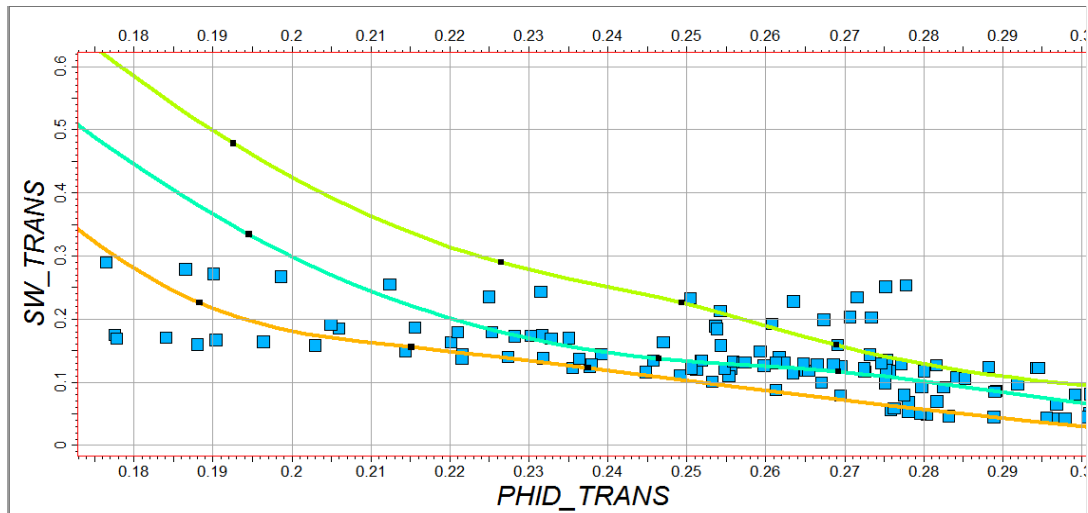


Figure 9: Transformation Plot for Reservoir B

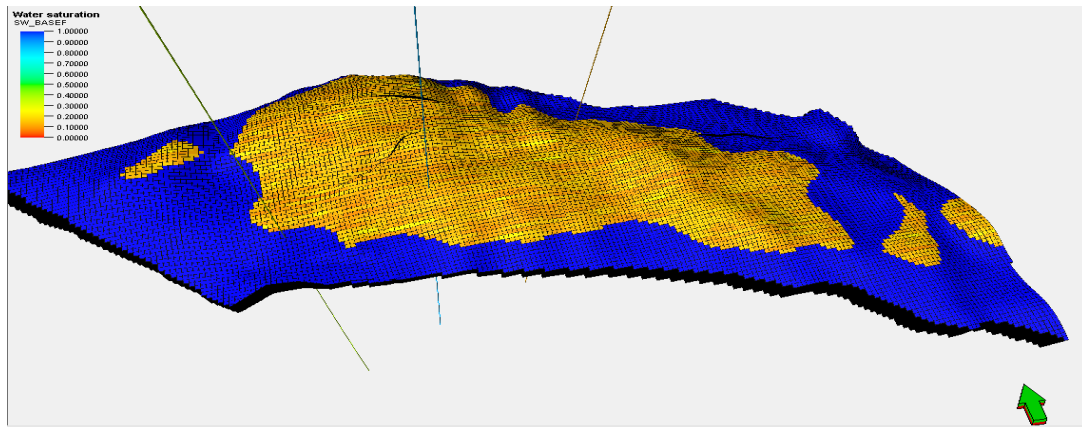


Figure 10: Water Saturation Model for Reservoir B

Reservoir B also has a moderate permeability. The fluid can move properly within the pore spaces. Reservoir C also shows similar result as reservoir B. It has an average effective porosity of 22% and a water saturation ranging from 17%-34% (figure 11 and figure 12). These results suggest that the pore spaces within this level is well connected. The fluid can move properly within the pore spaces.

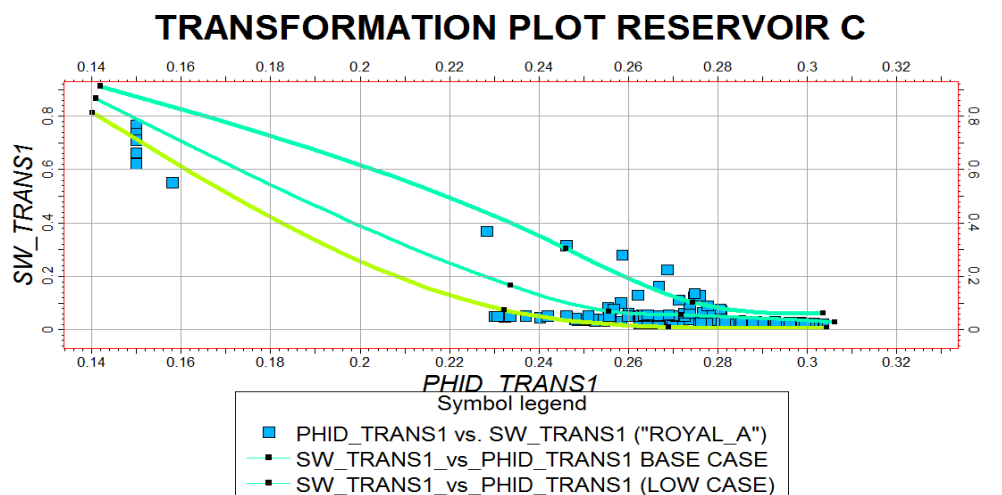


Figure 11: Transformation plot for Reservoir C

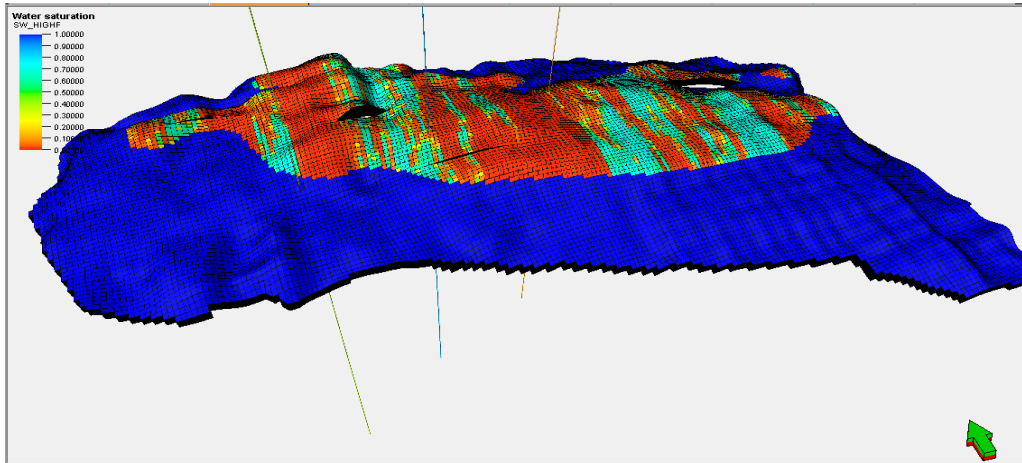


Figure 12: Water Saturation Model for Reservoir C

ROCK PHYSICS

From the Lambdarho-Murho crossplots (Figure 13) for Wells C and A, it could be observed that majority of the points were observed to fall within the shale (black ellipse) and brine (yellow ellipse) zones while the rest were observed within the oil (Blue ellipse) and Gas Zones (Red ellipse). Well D however showed a slightly different distribution of points on the plot as shown below in Figure 13. Majority of the points fall within the shale and brine zone while the rest within the hydrocarbon zone and hence the production from this well is expected to be considerably low.

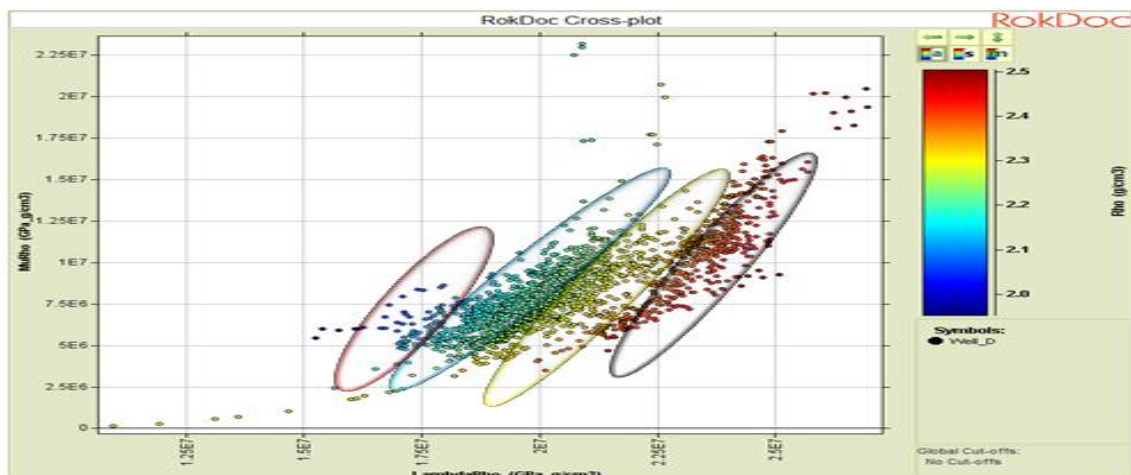


Figure 13: Lambdarho-Murho Cross-plot for Well D

The Lambdarho-Velocity Ratio Cross-plots (Figure 14) produced similar results with the same type of distribution of points within the plot. Black ellipse represented the shale zone, yellow ellipse represented the brine zone, blue ellipse represented the zone predominantly oil while red ellipse represented the gas zone.

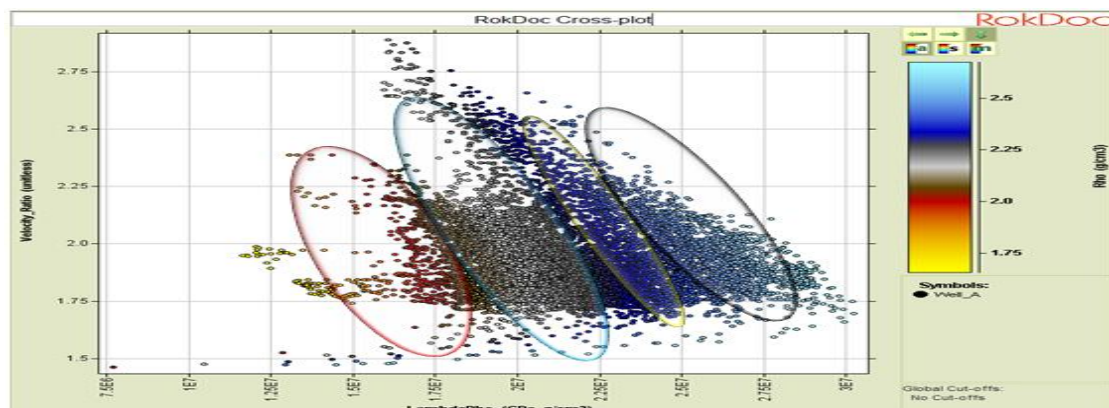


Figure 14: Lambdarho-Velocity Ratio Cross-plot

From Figure 15 below, it could be observed that majority of the points on the plots were observed to cluster around the friable sand model from which it could be inferred that the degree of cementation is substantially low within the reservoirs and this can be attributed partially to the significantly low clay content within the reservoirs. Below is a cross-plot of Compressional Velocity-Porosity from Reservoir B across well C (Royal C). An almost similar distribution was observed in other wells.

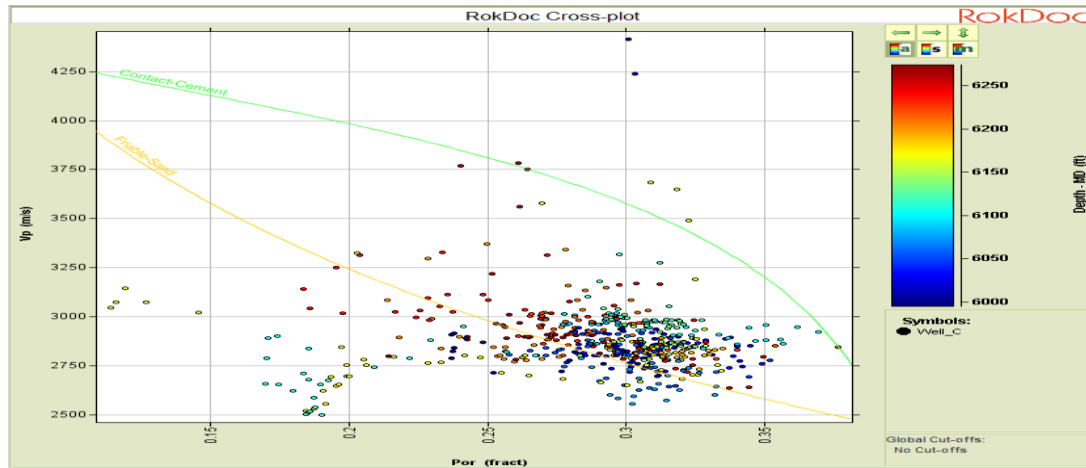


Figure 15: V_p – Porosity Cross-plot for Reservoir B across Well C.

From Figure 16 below, it could be observed that a substantial amount of the points on the cross-plot indicates that the lithology in the reservoir is almost totally sand with an API value of less than 40 as shown by the GR indicator.

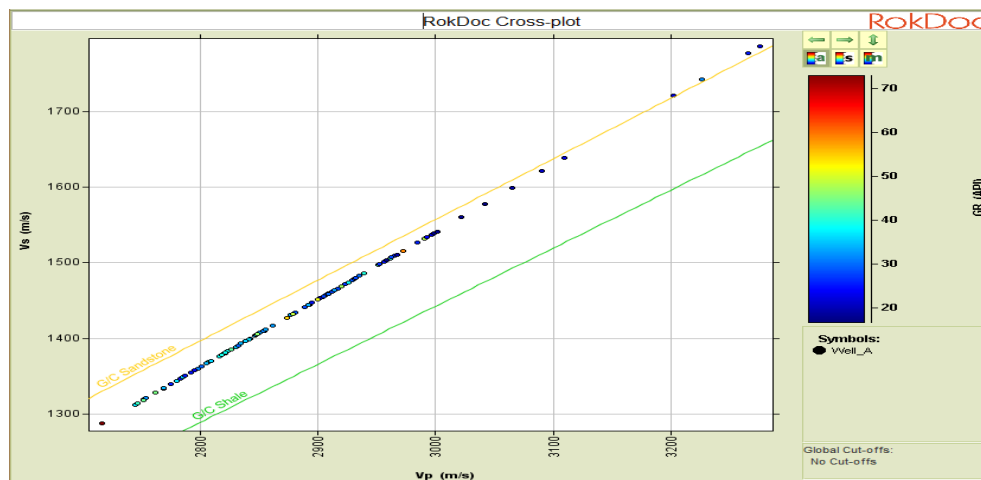


Figure 16: V_p – V_s Cross-plot for Reservoir C across Well A

VIII. Conclusion

The petrophysical analysis of the field indicate that reservoir B and C has an average effective porosity of 20% and 22% respectively. This shows that the pore spaces within the reservoir are well connected initially. The water saturation of these reservoirs (reservoir B ranges from 10%-22% while reservoir C ranges from 17%-34%) also indicate that the reservoirs are saturated with hydrocarbon. This suggest that the reservoirs can be exploited. Also, from the V_p – Porosity Cross-plot, it could be observed that the reservoir is poorly cemented and hence the connectivity of the pore spaces is likely to be seriously affected in the nearest future. Also, the trapping system appears to be an anticline and from the Lambdarho-Murho cross-plot, the amount of hydrocarbon in the reservoirs seems to increase from well D to A and then C (Towards the South West). Based on these, any future well to be drilled should be drilled in the same direction towards the edge of the anticline. The production can further be enhanced after a period of production time by employing reservoir geophysics monitoring tools. Time-lapse (4D) seismic which will give further reservoir monitoring and serves as a multi-disciplinary platform for efficient reservoir development is recommended for this field after a period of production. This will help in monitoring the effect of production on the connectivity of the pore spaces and further locating any other bypassed hydrocarbon zones on the field.

References

- [1]. Abe S.J, Olowokere MT. (2013). Reservoir characterization and formation evaluation of some parts of Niger delta using 3D seismic and well log data. *Research Journal in Engineering and Applied Sciences*. 2013;2(4):304-307.
- [2]. Ailin, J., Dongbo H, (2012). Advances and the challenges of reservoir characterization; a review of the current state-of-the-art earth sciences.
- [3]. Alistair R. Brown (2004). *Interpretation of Three-Dimensional Seismic Data* (6th Ed.). The American Association of Petroleum Geologists and the Society of Exploration Geophysicists Tulsa, Oklahoma, U.S.A.
- [4]. Amigun J.O., Olisa B. and Fadeyi O.O. (2012). Petrophysical analysis of well logs for reservoir evaluation: A case Study of 'Laja' Oil Field, Niger Delta. *Journal of Petroleum and Gas Exploration Research* (ISSN 2276-6510) Vol. 2(10) pp. 181-187. <http://www.interestjournals.org/JPGER>
- [5]. Doust H, Omatsola E (1990) Niger Delta, Divergent/passive margin basins. *American Association of Petroleum Geologists* 239-248.
- [6]. Edigbue; A.A. Komolafe; A.A. Adesida and O.J Itamuko (2014). Hydrocarbon reservoir characterization of "Keke" field, Niger Delta using 3 seismic and petrophysical data. *Research American Journal of Scientific and Industrial*. doi:10.5251/ajsir.2014.5.2.73.80. *Petroleum & Coal* 55 (1) 37-43, 2013. ISSN 1337-70
- [7]. Kearey, Philip (2001). *Dictionary of Geology* (2nd Ed.) London, New York, etc.: Penguin Reference, London, p. 123. ISBN 978-0-14-051494-0.
- [8]. Lukumon Adeoti, Njoku Onyekachi, Olawale Olatinsu, Julius Fatoba, Musa Bello (2014). Static Reservoir Modeling Using Well Log and 3-D Seismic Data in a KN Field, offshore Niger Delta, Nigeria. *International Journal of Geosciences*, 2014, 5, 93-106 Published Online January 2014 (<http://www.scirp.org/journal/ijg>) <http://dx.doi.org/10.4236/ijg.2014.51011>
- [9]. Michele L. W. Tuttle, Ronald R. Charpentier, and Michael E. Brownfield (1999). *The Niger Delta Petroleum System: Niger Delta Province, Nigeria, Cameroon, and Equatorial Guinea, Africa*. Denver, Colorado. U.S. Department of the Interior and Geological Survey
- [10]. Nwankwo C. N., Anyanwu. J and Ugwu S. A. (2014). Integration of Seismic and Well Log Data for Petrophysical Modeling of Sandstone Hydrocarbon Reservoir in Niger Delta. *Scientia Africana* (ISSN 1118 – 1931), Vol. 13 (No.1), June 2014. Pp186-199.
- [11]. Oluwadare OA, Osunrinde OT, Abe SJ, Ojo BT (2017) 3-D Geostatistical Model and Volumetric Estimation of 'Del' Field, Niger Delta. *J Geol Geophysics* 6: 291. doi: 10.4172/2381-8719.1000291.
- [12]. Schlumberger. (1989). *Log Interpretation, Principles and Application*. Schlumberger Wireline and Testing: Houston, TX. 21-89
- [13]. Stacher P (1995) Present understanding of the Niger Delta hydrocarbon habitat. *Geology of Deltas*: Rotterdam, Balkema AA, pp: 257-267.

Acknowledgment

Sincere appreciations go to Prof. (Mrs) M.T Olowokere, the shell professor of Geophysics, OAU Ile Ife, for providing data used for this study. Also, the department of Applied Geophysics, FUTA is greatly appreciated for the provision of Petrel 9.0 and Rock Doc. software used for the interpretation.

B.T Ojo. " Quantitative Modeling of the Architecture and Connectivity Properties of Reservoirs in 'Royal' Field, Niger-Delta.." *IOSR Journal of Applied Geology and Geophysics* (IOSR-JAGG) 6.2 (2018): 01-10.